

The X-ray eclipse of OY Car resolved with XMM-Newton: X-ray emission from the polar regions of the white dwarf

Peter J. Wheatley and Richard G. West

Department of Physics and Astronomy, University of Leicester, University Road, Leicester, LE1 7RH

8 November 2018

ABSTRACT

We present the XMM-Newton X-ray eclipse lightcurve of the dwarf nova OY Car. The eclipse ingress and egress are well resolved for the first time in any dwarf nova placing strong constraints on the size and location of the X-ray emitting region. We find good fits to a simple linear eclipse model, giving ingress/egress durations of 30 ± 3 s ($\Delta\phi_{\text{orb}} = 0.0055 \pm 0.0006$). Remarkably this is shorter than the ingress/egress duration of the sharp eclipse in the optical as measured by Wood et al. (1989) and ascribed to the white dwarf (43 ± 2 s). We also find that the X-ray eclipse is narrower than the optical eclipse by 14 ± 2 s, which is precisely the difference required to align the second and third contact points of the X-ray and optical eclipses. We discuss these results and conclude that X-ray emission in OY Car most likely arises from the polar regions of the white dwarf.

Our data were originally reported by Ramsay et al. (2001b), but they did not make a quantitative measurement of eclipse parameters. We have also corrected important timing anomalies present in the data available at that time.

Key words: Accretion, accretion disks – Binaries: eclipsing – Stars: novae, cataclysmic variables – Stars: individual: OY Car – X-rays: stars.

1 INTRODUCTION

X-ray eclipses have now been observed in three dwarf novae in quiescence (Wood et al. 1995; Mukai et al. 1997; Van Teeseling 1997; Pratt et al. 1999). The eclipses are deep, narrow, and centred on the white dwarf, providing strong evidence that the boundary layer is the source of the X-ray emission. The boundary layer is the region in which accretion disc material settles from its Keplerian velocity onto the surface of the white dwarf, giving up some of its kinetic energy (e.g. Pringle & Savonije 1979).

The most powerful X-ray eclipse study to date is of HT Cas with ASCA (Mukai et al. 1997). Mukai et al. made a detailed investigation of the eclipse depth, width and shape, and concluded that the eclipse is centered on the white dwarf, consistent with being total, and sufficiently sharp to limit the extent of X-ray emission to 1.15 the radius of the white dwarf.

Eclipsing dwarf novae are quite rare, and tend to be fainter in X-rays than their low-inclination counterparts (Van Teeseling & Verbunt 1994), so eclipse studies to date have been count-rate limited. HT Cas is the brightest eclipsing dwarf nova, and yet the ASCA data did not resolve the ingress and egress of the eclipse. Thus Mukai et al. were un-

able to measure the size or geometry of the X-ray emitting region.

In this paper we present the first XMM-Newton observations of an eclipsing dwarf nova: OY Car. The high effective areas of the XMM EPIC cameras allow us to resolve the ingress/egress of an X-ray eclipse for the first time. Our data have previously been reported by Ramsay et al. (2001b) and Ramsay et al. (2001a), but those authors did not attempt to make a quantitative measurement of the eclipse parameters, partly because of important timing anomalies that were present in the data available at that time. We have corrected these anomalies, and the resulting lightcurves allow us to place tight constraints on the size and location of the X-ray emitting region in OY Car.

Quiescent X-ray eclipses were discovered in OY Car with ROSAT by Pratt et al. (1999). The eclipse is narrow, deep and centred on the white dwarf, but the ROSAT observation did not yield enough counts for further analysis.

2 OBSERVATIONS

2.1 XMM-Newton EPIC X-ray data

OY Car was observed with XMM-Newton (Jansen et al. 2001) for 51 ks on 2000 June 29/30 (JD 2 451 725) shortly

arXiv:astro-ph/0307436v1 24 Jul 2003

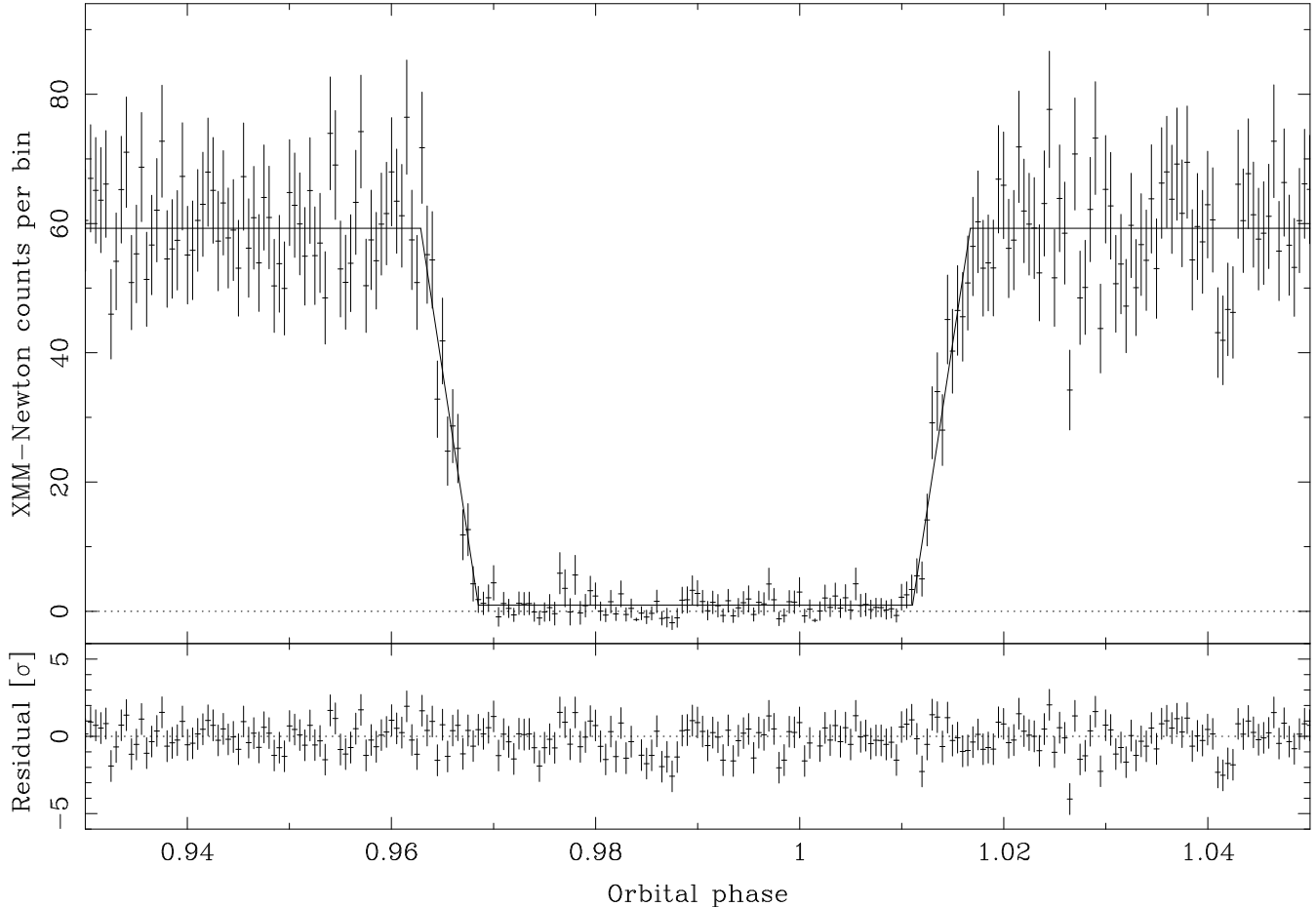


Figure 1. Folded XMM-Newton eclipse lightcurve of OY Car from the June 2000 observation. Data from the three EPIC X-ray cameras have been co-added, binned into 2000 phase bins, and the eclipse fitted with a simple piecewise linear model. The ingress/egress duration is found to be $29.5 \pm_{2.4}^{2.8}$ s, which is substantially shorter than the eclipse of the white dwarf observed in the optical/ultraviolet.

after an outburst. The data have been presented previously by Ramsay et al. (2001b) but suffered from two serious anomalies at that time. First, the absolute timing of all lightcurves were unknown. Thus the relative timing between the XMM-Newton cameras was unknown and Ramsay et al. were forced to align the lightcurves by eye. Second, there was a timing anomaly in the EPIC-pn lightcurve, caused by an onboard counter overflow, after which all events were offset by ~ 300 s. Ramsay et al. rejected events after this time.

We correct both these anomalies and combine data from all three EPIC cameras. Rather than extracting binned lightcurves and then folding these to produce a mean eclipse profile, we extract event lists for circular regions around OY Car and produce a folded lightcurve by calculating orbital phase for each event. This avoids the need to calculate errors on lightcurves with small numbers of counts per bin. Source counts were extracted from circles with 44 arcsec radius in the MOS cameras and 60 arcsec in the pn camera. Background counts were collected from 44 to 88 arcsec annuli in the MOS cameras, and the whole of the rest of the CCD was used in the pn camera (except the first ten rows, which are dominated by electronic noise). We produced two background-subtracted folded lightcurves, one with 1000 and one with 2000 phase bins. Throughout this

paper we use the ephemeris of Pratt et al. (1999) in which the orbital period of OY Car is 5453.64732 ± 0.00002 s. The eclipse profile from the 2000-bin lightcurve is presented in Fig. 1. In total, 10 eclipses were covered with all three EPIC cameras. It can be seen that the eclipse is occurring around one minute earlier than predicted by the ephemeris of Pratt et al. (1999). We find the centre of eclipse occurs at an orbital phase of 0.9898 ± 0.0004 . This difference is much greater than the stated error on the ephemeris and we can find no mistake in our phase calculation. XMM-Newton times are in the Terrestrial Time system (TT) and we have applied a heliocentric correction of +91 s to our lightcurve.

A second XMM-Newton observation of OY Car was made on 2000 August 7 (JD 2 451 764) lasting 14 ks. We reduced the X-ray data by the method described above and plot the folded eclipse lightcurve in the lower panel of Fig. 2. Three eclipses were covered with the two EPIC-mos cameras and two eclipses were covered with the EPIC-pn camera. A heliocentric correction of -23 s was applied to the XMM-Newton TT event times, yielding a phase offset that is consistent with that of the June observation.

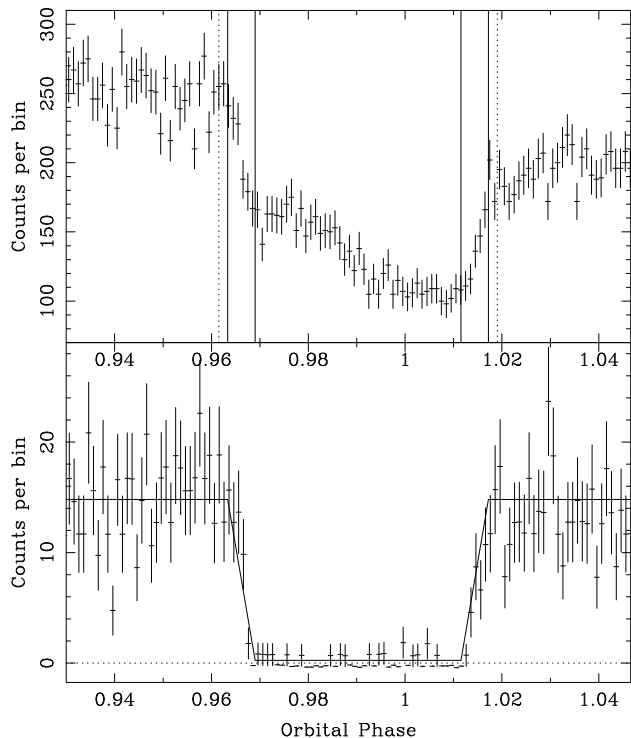


Figure 2. Folded XMM-Newton eclipse observations of OY Car from the second observation in August 2000. The top panel shows a fold of 3 OM eclipse observations with the B filter. The bottom panel shows a fold of 3 eclipse observations with the EPIC-mos X-ray cameras and 2 eclipse observations with the EPIC-pn camera. The solid curve plotted over the X-ray data represents our best fit to the June 2000 data from Fig. 1 (scaled by count rate). The solid vertical lines on the OM panel represent our measured X-ray contact points, and the dotted lines represent the separation of the first and fourth contact points of the white dwarf as derived by Wood et al. (1989) from ground-based optical observations. Both data sets are binned into 1000 orbital phase bins, corresponding to 5.5 s per bin.

2.2 XMM-Newton Optical Monitor data

The XMM-Newton Optical Monitor (OM; Mason et al. 2001) provides simultaneous optical or ultraviolet coverage of the EPIC field of view. The first XMM-Newton observation of OY Car was also the commissioning observation for the OM *fast mode*, in which high time resolution lightcurves can be accumulated. Unfortunately only two of the ten eclipses are covered by OM fast mode exposures, and the first of these suffers from a timing anomaly that we cannot recover. An eclipse lightcurve has been extracted from the second exposure and is plotted in the upper panel of Fig. 3. The observation was made using the UVW1 filter with a bandpass of approximately 250–350 nm. The lower panel of Fig. 3 shows the combined EPIC X-ray lightcurve for the same time interval.

By the time of the second XMM-Newton observation the OM fast mode was fully operational and an OM lightcurve is available for all three eclipses. The folded lightcurve is plotted in the upper panel of Fig. 2. This observation was made using the B filter with a bandpass of approximately 380–500 nm.

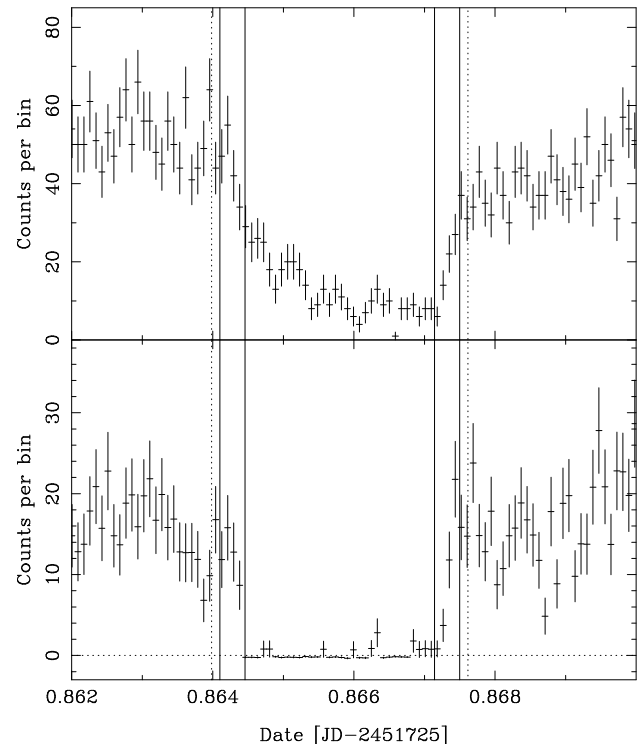


Figure 3. Simultaneous eclipse observation of OY Car with the UVW1 filter of the XMM-Newton OM (top) and the EPIC X-ray cameras (bottom). This is the only eclipse from the first XMM-Newton observation (June 2000) for which an OM lightcurve can be recovered with full timing information. The solid vertical lines indicate the X-ray contact points derived from our fit to the full folded lightcurve. The dotted vertical lines indicate the separation of the first and fourth contact points of the white dwarf derived by Wood et al. (1989) from ground-based optical observations. The bin size is 6.7 sec in both panels.

3 RESULTS

3.1 X-ray lightcurves

We fit the XMM-Newton eclipse lightcurve of OY Car using a simple piecewise linear model. Our model has five parameters: the ingress/egress duration, the phase of mid eclipse, the eclipse width (measured between mid ingress and mid egress), and the eclipse and out-of-eclipse count rates.

We first applied this model to the 1000-bin lightcurve of the June 2000 observation, in which there are sufficient counts in all bins to allow us to apply the χ^2 statistic. We fitted the 140 bins around mid-eclipse, and found an excellent fit with χ^2 of 135 and 135 degrees of freedom.

The estimated errors on the ingress/egress duration in this fit are dominated by the large bin size (≈ 5.5 s), and so we use the 2000-bin lightcurve for parameter estimation. We first fitted the 280 bins around mid-eclipse using the χ^2 statistic, in order to find an approximate fit. We did not use this fit to estimate errors because many eclipse bins contain too few counts. Instead we refitted the lightcurve using the Cash statistic (Cash 1979). This does not allow us test goodness of fit, but does allow us to estimate allowed parameters ranges in the same way as with χ^2 .

Our best Cash-statistic fit to the 2000-bin eclipse

lightcurve is plotted in Fig. 1. The residuals show no systematic effects during ingress or egress, and we are satisfied a linear fit is sufficient to characterise our eclipse data. Fitting with more complex models appears not to be warranted. Our best-fitting ingress/egress duration is 29.5 ± 2.8 s and the eclipse duration is 262.3 ± 1.4 s (68 per cent confidence intervals). The allowed ranges at 99 per cent confidence are 25.2–36.5 s and 259.1–266.3 s respectively.

Figure 4 shows our best-fit model overlaid on all of the individual eclipse ingress and egress phases from the June 2000 observation. It is clear that our model is also a good representation of the individual eclipses.

The folded X-ray lightcurve from the August 2000 observation is plotted in the lower panel of Fig. 2, with our best fit to the June data overlaid (scaled by count rate). The August observation is shorter and the source fainter than in June, but it can be seen that the model fit to the June data is an excellent representation of the August data. The X-ray eclipse lightcurve of OY Car seems therefore to be stable on timescales of months as well as hours.

3.2 Optical/UV lightcurves

Figure 2 shows the folded B-band eclipse lightcurve covering three eclipses during the August 2000 observation. Figure 3 shows the UVW1 eclipse lightcurve of a single eclipse during the June 2000 observation. These simultaneous observations confirm that the optical/UV eclipse is aligned with the X-ray eclipse and that the X-ray, optical and UV eclipse ingress and egress occur on very similar timescales. However, the low number of eclipses covered and the relatively small aperture of the OM do not allow us to constrain the eclipse parameters as tightly as earlier ground based observations.

4 DISCUSSION

4.1 Size and location of the X-ray emitting region

For the first time we have resolved the ingress and egress of an X-ray eclipse in a dwarf nova. The duration and timing of these transitions place tight constraints on the size and location of the X-ray emitting region, while their shape constrains the distribution of X-ray emitting plasma.

Our simple piecewise linear fit to the eclipse results in an excellent fit, with no systematic residuals (Fig. 1). We summarise our fitted eclipse parameters in Table 1, and include values taken from the optical study of Wood et al. (1989) for comparison.

Our model does not define a unique geometry, but corresponds to gas distributions in which an equal emission measure is occulted per unit time (or phase) by the limb of the secondary star. This is a fairly good approximation, for example, to an optically-thin boundary layer (see e.g. curve 3(c) in Fig. 2 of Wood & Horne 1990).

Remarkably our measured ingress/egress duration, 30 ± 3 s, is substantially less than that measured in the optical by Wood et al. (1989), 43 ± 2 s. If one assumes the optical contact points represent the contact points of the white dwarf then the X-ray emitting region must have a smaller extent than the white dwarf.

Even more remarkably, our measured X-ray eclipse

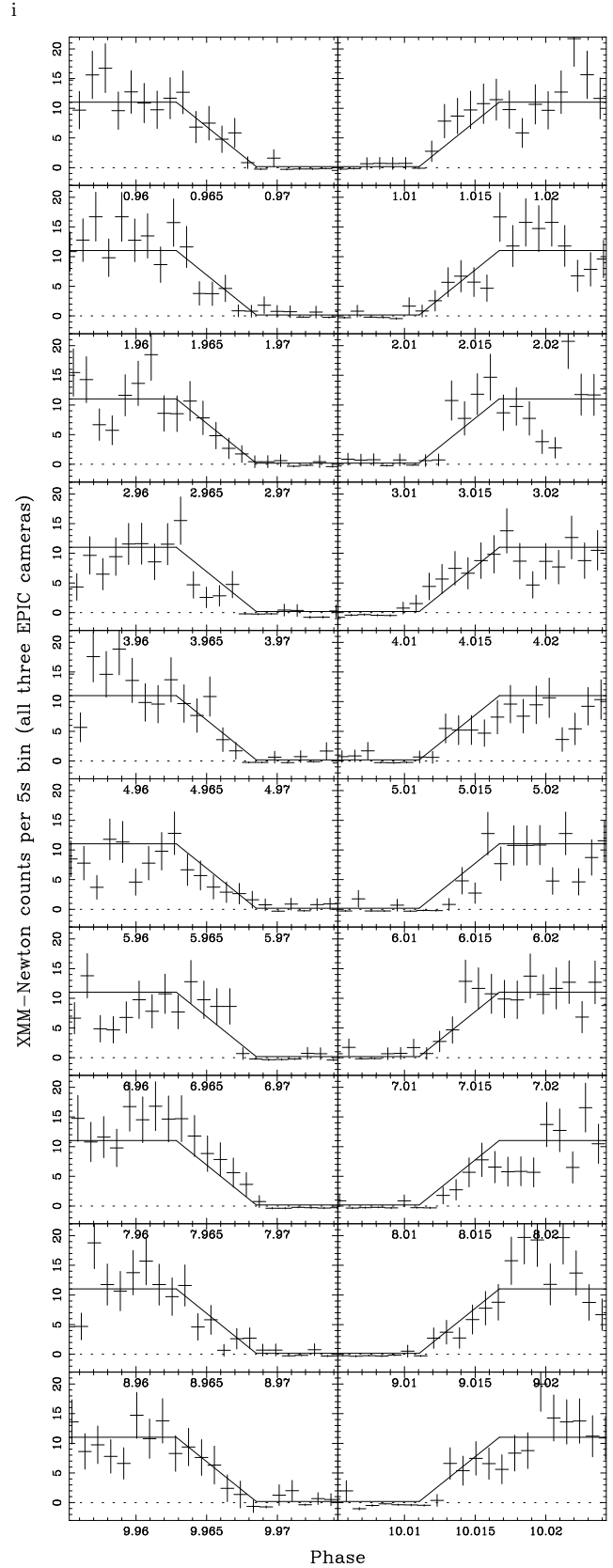


Figure 4. The full set of eclipse ingress and egress phases from the June 2000 XMM-Newton observation of OY Car. The solid line shows the best fit to the full folded lightcurve plotted in Fig. 1. It is clear that the same fit is also a good representation of the individual eclipses.

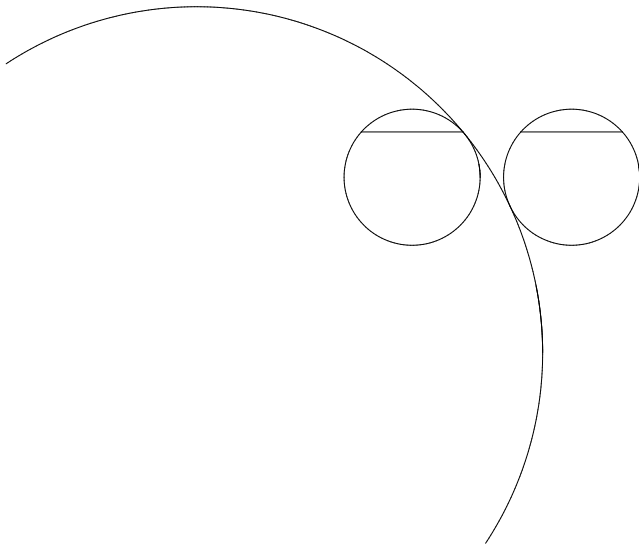


Figure 5. Schematic diagram of the eclipse of the white dwarf in OY Car, showing the first and second contact points of the white dwarf. The radius of the white dwarf has been increased by a factor three for clarity. It can be seen that the eclipse of X-rays emitted from the polar region will begin after the start of the optical ingress, but the end of ingress will occur simultaneously in both wavebands. The same behaviour will occur in reverse during egress. The duration of the X-ray eclipse (measured at the half-flux points) will also be shorter than in the optical band.

width, 262 ± 1 s, is also shorter than the optical eclipse measured by Wood et al. (1989), 276 ± 2 s. While the ingress/egress duration depends on the size of the emitting region, the eclipse duration is sensitive only to the size of occulting object. A narrower eclipse in X-rays implies that the secondary star must be narrower along our line of sight to X-ray emission than it is along our line of sight to the optical emission region. Since the scale height of the atmosphere of the secondary star is negligible with respect to the size of the white dwarf (e.g. Wood & Horne 1990), this situation can arise only if the X-ray emitting region is physically displaced vertically with respect to the centre-of-light in the optical.

The difference between the eclipse durations in the X-ray and optical bands, 14 ± 2 s, is precisely that required to align the second and third contact points of the X-ray and optical lightcurves. Assuming the X-ray and optical eclipses are centred on each other, the optical eclipse must begin before and finish after the X-ray eclipse. However, the point at which the eclipse becomes total, and the beginning of the egress from eclipse must be aligned in the two wavebands. This implies that, although the X-ray emitting region is vertically displaced with respect to the optical emission of the white dwarf, the X-ray emission does not extend beyond the limb of the white dwarf.

The combination of these constraints leads us to believe that we are seeing X-ray emission only from the upper polar region of white dwarf. Figure 5 shows a schematic of an eclipse in which the X-ray emission is displaced to the pole of the white dwarf. System parameters have been taken from Wood et al. (1989), but the radius of the white dwarf has been increased by a factor three for clarity. It can be

Table 1. Comparison of the eclipse parameters of OY Car from this work (X-rays) and from Wood et al. (1989; optical). Δ_{wi} and Δ_{we} are the durations of the eclipse ingress and egress respectively. $\Delta\phi$ is the width of the eclipse from mid-ingress to mid-egress. ϕ_0 is the phase of mid eclipse. All values are expressed in orbital phase.

		Δ_{wi}	Δ_{we}	$\Delta\phi$	ϕ_0
This work	best fit	0.0054		0.0481	0.9898
	1- σ error	0.0005		0.0003	0.0004
Wood et al. (1989)	mean	0.0077	0.0079	0.0506	0.0000
	rms	0.0004	0.0003	0.0004	0.0003

seen that such an arrangement would reproduce the implied phasings of the X-ray and optical eclipses of OY Car.

4.2 Origin of the vertical displacement

X-ray emission is not usually associated with the polar regions of the white dwarfs in dwarf novae, with most authors expecting emission from a narrow equatorial boundary layer between accretion disc and white dwarf. Emission from polar regions *is* seen in intermediate polars, where a strong magnetic field truncates the accretion disc and channels the accretion flow onto the magnetic poles of the white dwarf. A similar geometry may exist in OY Car, and this would represent the first discovery of magnetic accretion in a classical dwarf nova. The discovery of a 37 min period in the XMM-Newton lightcurve by Ramsay et al. (2001b) may support this interpretation, although this is a relatively long spin period for an intermediate polar. Alternatively we can imagine geometries in which the entire white dwarf surface is covered by X-ray emitting material, but that the equatorial regions are obscured by material that is optically thick in the X-ray band but optically thin in the optical. In both interpretations the observed asymmetry leading to the apparent vertical displacement of the X-ray emitting region requires that any X-ray emission from the lower hemisphere of the white dwarf must be obscured. This obscuration can probably be attributed to the accretion disc itself.

4.3 The white dwarf eclipse

Our conclusion that the X-ray emitting region has a smaller extent than the white dwarf depends critically on the assumption that the optical contact points measured by Wood et al. (1989) accurately represent the contact points of the white dwarf. In a second paper Wood & Horne (1990) use realistic white dwarf and boundary layer models to fit the eclipse shape and find the beginning and end of ingress/egress are too gradual to be fitted with a white dwarf filling the contact points of Wood et al. (1989), even with maximum limb darkening. As a result, their fitted white-dwarf radii ($0.0144a$ – $0.0163a$) are smaller than that from the direct contact-point measurement ($0.0182a$) implying a white-dwarf ingress/egress with the same duration as we find in X-rays.

Wood & Horne (1990) discuss this discrepancy and conclude that it can be resolved by one of two possibilities: 1)

the direct method of contact point measurement employed by Wood et al. (1989) may suffer from a bias that leads to an over-estimate of the size of the white dwarf; or 2) the range of models considered by Wood & Horne (1990) may not include a model that adequately describes the intensity distribution of the central object in OY Car. They go on to suggest that a white dwarf model with a bright equatorial region that has a large extent in latitude might allow an acceptable fit with a white dwarf radius as large as that measured by Wood et al. (1989).

Given this uncertainty in the appropriate model for the central object in OY Car, we believe that the direct contact-point method of Wood et al. (1989) is probably a more reliable method for defining the contact points of the white dwarf than the fitting of Wood & Horne (1990). If one accepts this view then the X-ray emission in OY Car most probably arises from the polar regions of the white dwarf. If one does not accept this view then the extent of the X-ray emitting region can be as large as the white dwarf. However, the width of the optical eclipse found by Wood et al. (1989) and Wood & Horne (1990) are consistent, and so the X-ray emitting region must still be displaced vertically with respect to the optical centre-of-light of the white dwarf.

5 CONCLUSIONS

For the first time we have resolved the X-ray ingress and egress of an eclipse in a dwarf nova. Comparison with high-precision ground-based optical observations has shown that the ingress/egress duration is substantially shorter in the X-ray band, implying the X-ray emitting region is smaller than the white dwarf (although see Sect. 4.3). The eclipse width is also smaller in the X-ray band, implying that the X-ray emitting region must be vertically displaced with respect to the centre of the white dwarf. The difference in ingress/egress duration, 13 ± 4 s, is consistent with the difference in the eclipse width, 14 ± 2 s. Assuming the X-ray and optical eclipses are centred at the same phase, this means that the second and third contact points must be aligned. Thus, although the X-ray emission is vertically displaced from the centre of the white dwarf, it cannot extend beyond the limb of the white dwarf. We therefore conclude that the X-ray emission in OY Car most likely arises from the upper polar region of the white dwarf. Any emission from the lower pole must be occulted, presumably by the accretion disc.

ACKNOWLEDGMENTS

We thank Janet Wood for useful discussions, and the referee Koji Mukai for spotting a serious error in the first version of this paper. Research in astrophysics at the University of Leicester is supported by PPARC rolling grants. This paper was based on observations obtained with XMM-Newton, an ESA science mission with instruments and contributions directly funded by ESA Member States and the US (NASA).

REFERENCES

- Cash, W., 1979, *ApJ*, 228, 939.
 Jansen, F., Lumb, D., Altieri, B., Clavel, J., Ehle, M., Erd, C., Gabriel, C., Guainazzi, M., Gondoin, P., Much, R., Munoz, R., Santos, M., Scharfel, N., Texier, D. & Vacanti, G., 2001, *A&A*, 365, L1.
 Mason, K. O., Breeveld, A., Much, R., Carter, M., Cordova, F. A., Cropper, M. S., Fordham, J., Huckle, H., Ho, C., Kawakami, H., Kennea, J., Kennedy, T., Mittaz, J., Pandel, D., Priedhorsky, W. C., Sasseen, T., Shirey, R., Smith, P. & Vreux, J.-M., 2001, *A&A*, 365, L36.
 Mukai, K., Wood, J. H., Naylor, T., Schlegel, E. M. & Swank, J. H., 1997, *ApJ*, 475, 812.
 Pratt, G. W., Hassall, B. J. M., Naylor, T. & Wood, J. H., 1999, *MNRAS*, 307, 413.
 Pringle, J. E. & Savonije, G. J., 1979, *MNRAS*, 187, 777.
 Ramsay, G., Cordova, F., Cottam, J., Mason, K., Much, R., Osborne, J., Pandel, D., Poole, T. & Wheatley, P., 2001a, *A&A*, 365, 294.
 Ramsay, G., Poole, T., Mason, K., Cordova, F., Priedhorsky, W., Breeveld, A., Much, R., Osborne, J., Pandel, D., Potter, S., West, J. & Wheatley, P., 2001b, *A&A*, 365, 288.
 Van Teeseling, A. & Verbunt, F., 1994, *A&A*, 292, 519.
 Van Teeseling, A., 1997, *A&A*, 319, L25.
 Wood, J. H. & Horne, K., 1990, *MNRAS*, 242, 606.
 Wood, J. H., Horne, K., Berriman, G. & Wade, R. A., 1989, *ApJ*, 341, 974.
 Wood, J. H., Naylor, T., Hassall, B. J. M. & Ramseyer, T. F., 1995, *MNRAS*, 273, 772.